

very high sulphate concentrations (Fig. 1). Thus, differences in P cycling between freshwaters and salt waters may also influence the switch in nutrient limitation.

A further implication of our findings is a possible effect of anthropogenic S pollution on P cycling in lakes. Our data indicate that aquatic systems with low sulphate concentrations have low RPR under either oxic or anoxic conditions; systems with only slightly elevated sulphate concentrations have significantly elevated RPR, particularly under anoxic conditions (Fig. 1). Work on the relationship between sulphate loading and

P release has yet to prove the mechanism behind this relationship. If sediment P release were controlled largely by sulphur, our view of the lakes that are being affected by atmospheric S pollution could be altered. It is believed generally that lakes with well-buffered watersheds are insensitive to the effects of atmospheric S pollution. However, because changing atmospheric S inputs can alter the sulfate concentration in surface waters²² independent of acid neutralization in the watershed, the P cycle of even so-called 'insensitive' lakes may be affected. □

Received 22 February; accepted 15 August 1987.

1. Bostrom, B., Jansson, M. & Forsberg, G. *Arch. Hydrobiol. Beih. Ergebn. Limnol.* **18**, 5-59 (1982).
2. Mortimer, C. H. *J. Ecol.* **29**, 280-329 (1941).
3. Hecky, R. E. & Kilham, P. *Limnol. Oceanogr.* **33**, 776-795 (1988).
4. Howarth, R. W. *A. Rev. Ecol. Syst.* **19**, 191-198 (1988).
5. Richards, F. A. in *Chemical Oceanography* (eds Riley, J. P. & Skirrow, G.) 601-645 (Academic, London, 1965).
6. Richards, F. A., Cline, J. D., Broenkow, W. W. & Atkinson, L. P. *Limnol. Oceanogr., Suppl.* **10**, R185-R202 (1965).
7. SenGupta, R. thesis, Univ. Goteborg, (1973).
8. Burns, N. M. & Ross, C. *Proc. 14th Conf. Great Lakes Research* 749-760 (1971).
9. Uehlinger, U. & Bloesch, J. *Freshwater Biology* **17**, 99-108 (1987).
10. Honjo, S., Manganini, S. J. & Cole, J. J. *Deep Sea Res.* **29**, 609-625 (1982).
11. Levine, S. N., Stainton, M. P. & Schindler, D. W. *Can. J. Fish. Aquat. Sci.* **43**, 366-378 (1986).
12. Hawke, D., Carpenter, P. D. & Hunter, K. A. *Envir. Sci. Technol.* **23**, 187-191 (1989).
13. Sugawara, K., Koyama, T. & Kamata, E. *J. Earth Sci., Nagoya Univ.* **5**, 60-67 (1957).
14. Stauffer, R. E. *Limnol. Oceanogr.* **30**, 123-146 (1985).
15. Gachter, R. & Mares, A. *Limnol. Oceanogr.* **30**, 364-371 (1985).
16. Lean, D. R. S., McQueen, D. J. & Story, V. A. *Arch. Hydrobiol.* **108**, 269-280 (1986).

17. Nurnberg, G. *Can. J. Fish. Aquat. Sci.* **43**, 574-580 (1985).
18. Curtis, P. *J. Nature* **337**, 156-158 (1989).
19. Carignan, R. & Tessier, A. *Geochim. cosmochim. Acta* **52**, 1179-1188 (1988).
20. Howarth, R. W. & Cole, J. J. *Science* **229**, 653-655 (1985).
21. Seitzinger, S. P., Nixon, S. W. & Pilson, M. E. Q. *Limnol. Oceanogr.* **29**, 73-83 (1984).
22. Likens, G. E. *Hydrobiologia* **176/177**, 331-348 (1989).
23. Brunskill, G. J., Povoleto, D., Graham, B. W. & Stainton, M. J. *Fish. Res. Bd Can.* **28**, 277-294 (1971).
24. Heaney, S. I., Smyly, W. J. P. & Talling, J. F. *Int. Rev. ges. Hydrobiol.* **71**, 441-494 (1986).
25. Gorham, E. & Swaine, D. J. *Limnol. Oceanogr.* **10**, 268-279 (1965).
26. Schelske, C. L. in *Biological Effects in the Hydrobiological Cycle* 59-81 (Purdue University, 1971).
27. Williams, J. D. H., Jaquet, J. M. & Thomas, R. L. *J. Fish. Res. Bd Can.* **33**, 413-429 (1976).
28. Menzel, D. W. & Corwin, N. *Limnol. Oceanogr.* **10**, 280-282 (1965).
29. Stainton, M. P. *J. Fish. Res. Bd Can.* **50**, 1441-1445 (1973).
30. Capone, D. G. & Liene, R. P. *Limnol. Oceanogr.* **33**, 725-749 (1988).

ACKNOWLEDGEMENTS. We thank S. Nolan, M. Pace, K. Porter, A. H. Puccoon and D. W. Schindler for advice and assistance. This project was supported by the NSF, the Andrew W. Mellon Foundation, and by the Mary Flagler Cary Charitable Trust, and is a contribution to the program of the Institute of Ecosystem Studies.

Routing of meltwater from the Laurentide Ice Sheet during the Younger Dryas cold episode

Wallace S. Broecker*, James P. Kennett†, Benjamin P. Flower‡, James T. Teller‡, Sue Trumbore§, Georges Bonani§ & Willy Wolfli§

* Lamont-Doherty Geological Observatory, Palisades, New York 10964, USA

† Marine Institute and Department of Geology, University of California, Santa Barbara, California 93106, USA

‡ Department of Geological Sciences, University of Manitoba, Winnipeg, Manitoba, Canada, R3T2N2

§ ETH Honggerberg, CH-8093 Zurich, Switzerland

ROTH¹ proposed that the Younger Dryas cold episode, which chilled the North Atlantic region from 11,000 to 10,000 yr BP, was initiated by a diversion of meltwater from the Mississippi drainage to the St Lawrence drainage system. The link between these events is postulated to be a turnoff, during the Younger Dryas cold episode, of the North Atlantic's conveyor-belt circulation system which currently supplies an enormous amount of heat to the atmosphere over the North Atlantic region². This turnoff is attributed to a reduction in surface-water salinity, and hence also in density, of the waters in the region where North Atlantic Deep Water (NADW) now forms. Here we present oxygen isotope and accelerator radiocarbon measurements on planktonic foraminifera from Orca Basin core EN32-PC4 which reveal a significant reduction in meltwater flow through the Mississippi River to the Gulf of Mexico from about 11,200 to 10,000 radiocarbon years ago. This finding is consistent with the record for Lake Agassiz which indicates that the meltwater from the southwestern margin of the Laurentide Ice Sheet was diverted to the northern Atlantic Ocean through the St Lawrence valley during the interval from ~11,000 to 10,000 years before present (yr BP).

Evidence for these diversions of meltwater comes from changes in the level of proglacial Lake Agassiz, which acted as a 'clearinghouse' for runoff from a $2 \times 10^6 \text{ km}^2$ area along the southwestern side of the Laurentide Ice Sheet³. Before 11,000 yr BP, the meltwater reaching Lake Agassiz overflowed to the Gulf of Mexico through the Mississippi River drainage system (Fig. 1a). By ~11,000 yr BP the Laurentide Ice Sheet had retreated far enough to open a series of channels leading to the Lake Superior basin, creating a diversion of the Agassiz

TABLE 1 Key radiocarbon dates of wood

Moorhead low-water phase of Lake Agassiz*	
10,960 ± 300 (W-723)	10,340 ± 170 (I-5213)
10,820 ± 190 (TAM-1)	10,200 ± 80 (GSC-1909)
10,680 ± 190 (GSC-677)	10,080 ± 280 (W-900)
10,550 ± 200 (Y-411)	10,050 ± 300 (W-1005)
Marquette glacial advance into Superior basin†	
10,250 ± 250 (W-1541)	10,100 ± 100 (WIS-409)
10,230 ± 300 (W-3896)	9,850 ± 300 (W-3866)
10,230 ± 500 (W-1414)	9,780 ± 250 (W-3904)
10,220 ± 215 (DAL-338)	9,730 ± 140 (I-5082)
10,200 ± 500 (M-359)	9,545 ± 225 (DAL-340)
10,100 ± 250 (WIS-409)	
Emerson high-water phase of Lake Agassiz‡	
10,000 ± 280 (GSC-1428)	9,890 ± 300 (I-4853)
10,000 ± 150 (GSC-870)	9,880 ± 225 (GX-3696)
9,990 ± 160 (GSC-391)	9,820 ± 300 (W-1361)
9,940 ± 160 (I-3880)	9,810 ± 300 (W-1360)
9,930 ± 280 (W-388)	9,700 ± 140 (GAC-797)
9,900 ± 400 (W-993)	

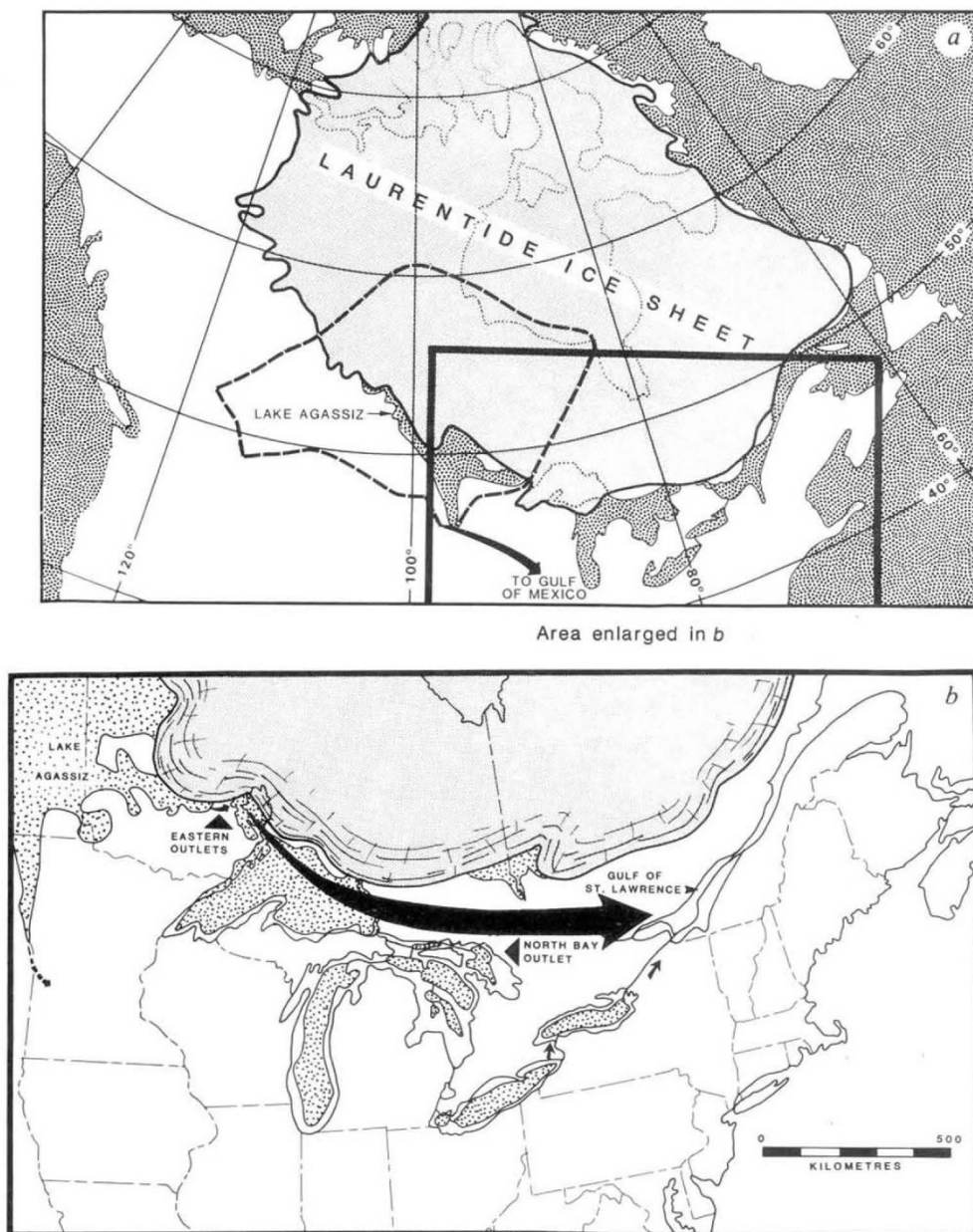
These dates (yr BP) were used to establish the chronology for the routing of meltwater from Lake Agassiz drainage basin during the Younger Dryas cold episode. The sample numbers are given in brackets.

* Low-water phase during which meltwater flowed east to the northern Atlantic Ocean.

† Glacial advance that dammed eastern overflow from Lake Agassiz.

‡ High-water phase during which meltwater flowed south to Gulf of Mexico.

FIG. 1 *a*, Map showing Laurentide Ice Sheet and routing of overflow from the Lake Agassiz basin (dashed outline) to the Gulf of Mexico just before the Younger Dryas^{22,23}; *b*, Routing of overflow from Lake Agassiz through the Great Lakes to the St Lawrence and northern Atlantic during the Younger Dryas²⁴.



water eastward through the Great Lakes and the St Lawrence valley to the northern Atlantic (Fig. 1*b*). Thus, during the Younger Dryas, meltwater and precipitation from the Lake Agassiz basin, the discharge of which is estimated⁴ to have been $\sim 30,000 \text{ m}^3 \text{ s}^{-1}$, was diverted to the northern Atlantic Ocean from its previous route to the Gulf of Mexico. This diversion caused the level of Lake Agassiz to drop by $\geq 40 \text{ m}$, creating the Moorhead low-water phase⁵. Radiocarbon dates of material from the portions of the floor of Lake Agassiz exposed during the Moorhead low-water phase range from 10,960 to 10,050 radiocarbon years (Table 1).

Drainage from Lake Agassiz was routed back to the Mississippi River and Gulf of Mexico beginning $\sim 10,000$ years ago, when ice of the Marquette glacial advance once again dammed the eastern overflow channels that had linked Lake Agassiz with the St Lawrence during the time corresponding to the Younger Dryas. Lake Agassiz again rose at this time to its Mississippi outlet initiating the Emerson high-water phase. Radiocarbon dates related to both the ice advance in the Superior basin and the Emerson high-water phase are shown in Table 1. Eleven radiocarbon ages for the ice re-advance range from 10,250 to

9,545 yr and average 10,020 yr. Eleven radiocarbon ages for the Emerson high-water phase of Lake Agassiz range from 10,000 to 9,700 yr.

An appropriate independent test for these reconstructions of drainage history is to date meltwater influx episodes to the Gulf of Mexico, recorded in the sedimentary record as negative values in the $\delta^{18}\text{O}$ of planktonic foraminifera^{12,13}. Because of bioturbation effects however, necessary resolution is not attainable for sediments that accumulate at rates of $8 \text{ cm per } 10^3 \text{ yr}$. The Orca Basin, located on the continental rise off Louisiana, not only offers high sedimentation rates ($50 \text{ cm per } 10^3 \text{ yr}$) but also anoxic conditions and hence a lack of sediment mixing¹⁴⁻¹⁷. There is^{14,15} a major negative $\delta^{18}\text{O}$ spike in Orca Basin core EN32-PC6. Accelerator radiocarbon dating of this core conducted on planktonic foraminifera¹⁸ revealed what seemed to be a sedimentation hiatus covering the time interval of the Younger Dryas. A more recent radiocarbon age of $10,910 \pm 160 \text{ yr}$ (or $10,500 \text{ yr}$ after correction for the $\sim 400\text{-yr}$ age for surface water ΣCO_2) for a new sample of mixed planktonic foraminifera from 436-437 cm depth in EN32-PC6, however, supports the contention that accumulation was continuous¹⁷.

Because of our original suspicion that a hiatus existed in EN32-PC6 we turned to a companion core, EN32-PC4, and determined the oxygen isotopic composition of both the white and pink variety of *Globigerinoides ruber* (Fig. 2). The isotope record was radiocarbon dated using the accelerator ^{14}C method (Table 2 and Fig. 2). Both ^{18}O records show the meltwater anomaly¹²⁻¹⁵. The white *G. ruber* record shows a sharp increase ($\sim 3\%$) in $\delta^{18}\text{O}$ at $\sim 11,000$ yr BP which is consistent with the cessation of meltwater flow expected from a diversion of the Lake Agassiz water. This increase is followed by a sharp decrease ($\sim 2\%$) in $\delta^{18}\text{O}$ at $\sim 10,000$ yr BP which is consistent with the rejuvenation of meltwater flow when the Lake Agassiz discharge was returned to the Mississippi River system.

Had we stopped with the analysis of the white variety of *G. ruber* we would have concluded that the evidence from the Gulf of Mexico is in full agreement with the expectation based on the Lake Agassiz record. The analyses of pink forms of *G. ruber*, however, complicates the situation. Although they show the major $\delta^{18}\text{O}$ increase corresponding to the eastward diversion 11,000 yr BP, they show no decrease at 10,000 yr BP. Rather, the $\delta^{18}\text{O}$ value remains nearly constant from 11,000 yr BP to present. Another puzzling contrast between these two records is that the $\delta^{18}\text{O}$ value for the white form of *G. ruber* is 1‰ higher than that for the pink form during glacial and Younger Dryas times, whereas the two forms yield similar values before and after Younger Dryas time. These differences are not easily explained. Net-tow¹⁹ plankton sampling and isotope²⁰ studies suggest that the pink form of *G. ruber* lives only during summer months, whereas the white form lives throughout the year. As the largest meltwater flux to the Gulf of Mexico would certainly have been during the summer months, this would be the least probable time for the Orca Basin to have been free of meltwater effects.

The important question here is whether the difference between the records invalidates our claim for verification of the cessation event. For example, a strong winter cooling ($\sim 6^\circ\text{C}$) during the Younger Dryas would explain the trough in the $\delta^{18}\text{O}$ record in white forms of *G. ruber*. In this case no increase in meltwater

TABLE 2 Radiocarbon dates of mixed planktonic shells

Sample No.	Depth (cm)	^{14}C age (yr)	Corrected ^{14}C age* (yr)
F120	94-96	9,100 \pm 190	8,700
F81	144-146	10,490 \pm 90	10,100
F82	150-152	10,700 \pm 130	10,300
F83	164-166	11,030 \pm 90	10,600
F84	192-196	11,510 \pm 100	11,100
F85	214-216	12,450 \pm 90	12,000
F121	288-290	12,900 \pm 150	12,500

These are the ages, determined by accelerator mass spectrometry at ETH Zurich, of mixed planktonic shells from Orca Basin core EN32-PC4 ($26^\circ 56.1' \text{ N}$, $91^\circ 21.7' \text{ W}$; 2,260 m).

* Corrected for air-sea $\Delta^{14}\text{C}$ difference.

flow down the Mississippi 10,000 yr BP would be required. Indeed, faunal data have been interpreted as indicating a cooling of the Gulf of Mexico during the Younger Dryas cold episode¹⁷. However, no support for a large cooling has been found in the pollen record for the southeastern United States (see ref. 21 for a summary).

Although it is unclear how much of the change in the $\delta^{18}\text{O}$ observed in the white form of *G. ruber* is due to reintroduction of meltwater and how much to a temperature increase, the chronology of the oxygen isotope record in the Gulf of Mexico seems to be in harmony with that for the record of Lake Agassiz. Although further tests of this hypothesis are required, the fact that the Younger Dryas interval is bracketed by dramatic oxygen isotope changes in the Gulf of Mexico is strong support for the proposal that a major influx in meltwater to the northern Atlantic ocean was responsible for the Younger Dryas cold episode.

Independent oxygen-isotope evidence from the Bay of Biscay (France) for benthic foraminifera²⁵ and a new coral-based chronology for the sea level during the time interval 15,000-9,000 yr BP²⁶ suggest that the Younger Dryas interval was one of reduced meltwater flow relative to the warm intervals before and after this event. The problem is that as meltwater from other sectors of the Laurentide Ice Sheet and from the Scandinavian Ice Sheet entered the Northern Atlantic at all times, it might be claimed that the increase in fresh-water input to the northern Atlantic at the onset of the Younger Dryas cold episode caused by the diversion of meltwater from the Mississippi to the St Lawrence was largely offset by a reduction in meltwater input from these other sectors. A further issue regarding the Rooth hypothesis is that the re-diversion of meltwater from the Mississippi to the St Lawrence after 10,000 yr BP failed to produce a cold event comparable to the Younger Dryas. Although we do not have satisfactory answers to these questions, we feel that the cadmium- and carbon-isotope data for benthic foraminifera²⁷ clearly show that the Atlantic conveyor-belt system did shut down during the Younger Dryas time. Taken together with meltwater-routine chronology we feel that the case for a diversion trigger remains strong. □

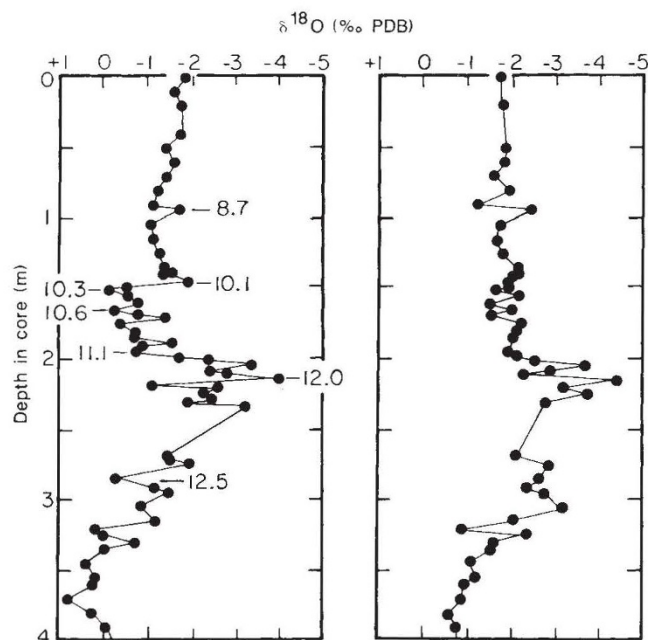


FIG. 2 Oxygen isotope changes in two varieties of *Globigerinoides ruber* (white and pink, left and right, respectively) from EN32-PC4 during latest Quaternary are plotted against depth. Ages shown are accelerator radiocarbon ages. Both varieties show a major 'meltwater spike' from ~ 320 -200 cm. *G. ruber* (white variety) shows increased $\delta^{18}\text{O}$ 1‰ relative to PDB standard values at the beginning of the Younger Dryas cold episode, consistently high values during the episode ($\sim 11,000$ -10,000 yr BP), and a sudden decrease at 10,000 yr BP termed the 'cessation event'.

Received 5 June; accepted 21 August 1989.

- Rooth, C. *Prog. Oceanogr.* **11**, 131-149 (1982).
- Broecker, W. S., Peteet, D. & Rind, D. *Nature* **315**, 21-25, 1985.
- Teller, J. T. & Clayton, L. in *Glacial Lake Agassiz, Spec. pap. 26* (Geological Association of Canada, Ottawa, 1983).
- Teller, J. T. in *The Late Quaternary Development of the Champlain Sea Basin, Spec. pap. 35*, 281-289 (Geological Association of Canada, Ottawa, 1988).
- Teller, J. T. & Thorleifson, L. H. in *Glacial Lake Agassiz, Spec. pap. 26*, 261-290 (Geological Association of Canada, Ottawa, 1983).
- Clayton, L. & Moran, S. R. *Quat. Sci. Rev.* **1**, 55-82 (1982).
- Moran, S. R., Clayton, L., Scott, M. & Brophy, J. *North Dakota Geol. Survey Miscellaneous Ser.* 53 (North Dakota Geological Survey, Pierre, 1973).
- Teller, J. T. *Geological Report GR80-4* (Manitoba Mineral Resources Division, Winnipeg, 1980).
- Drexler, C. W., Farrand, W. & Hughes, J. in *Glacial Lake Agassiz, Spec. pap. 26*, 309-329 (Geological Association of Canada, Ottawa, 1983).
- Clayton, L. in *Glacial Lake Agassiz, Spec. pap. 26*, 291-307 (Geological Association of Canada, Ottawa, 1983).

11. Arndt, B. M. *Rep. of Investigation No. 60* (North Dakota Geological Survey, Pierre, 1977).
 12. Kennett, J. P. & Shackleton, N. J. *Science* **188**, 147–150 (1975).
 13. Emiliani, C. *et al. Science* **189**, 1083–1088 (1975).
 14. Leventer, A., Williams, D. F. & Kennett, J. P. *Earth planet. Sci. Lett.* **59**, 11–17 (1982).
 15. Leventer, A., Williams, D. F. & Kennett, J. P. *Mar. Geol.* **53**, 23–40 (1983).
 16. Kennett, J. P. & Penrose, N. L. *Nature* **276**, 172–173 (1978).
 17. Kennett, J. P., Elmstrom, K. & Penrose, N. *Palaeogeogr. Palaeoclimatol. Palaeoecol.* **50**, 189–216 (1985).
 18. Broecker, W. S. *et al. Paleoceanography* **3**, 1–19 (1988).
 19. Be, A. W. H. *Micropaleontology* **6**, 373–392 (1960).
 20. Tolderlund, D. S. & Be, A. W. H. *Micropaleontology* **17**, 297–329 (1971).
 21. Rind, D., Peteet, D., Broecker, W., McIntyre, A. & Ruddiman, W. *Clim. Dyn.* **1**, 3–33 (1986).
 22. Dyke, A. S. & Prest, V. K. *Geogr. phys. Quat.* **41**, 237–263 (1987).
 23. Teller, J. T. in *Quaternary Evolution of the Great Lakes, Spec. pap. 30*, 1–16 (Geological Association of Canada, Ottawa, 1985).
 24. Teller, J. T. in *Geology of North America* vol. K-3 (eds Ruddiman, W. F. and Wright, H. E.) (Geological Society of America, Boulder, 1987).
 25. Duplessy, J.-C., Delibrias, G., Turon, G., Pujol, C. & Duprat, J. *Palaeogeogr. Palaeoclimatol. Palaeoecol.* **35**, 121–144 (1981).
 26. Fairbanks, R. G. *Nature* (in the press).
 27. Boyle, E. A. & Keigwin, L. *Nature* **330**, 35–40 (1987).
 28. Rind, D., Peteet, D., Broecker, W., McIntyre, A. & Ruddiman, W. *Clim. Dyn.* **1**, 3–33 (1986).

ACKNOWLEDGEMENTS. We acknowledge the financial support of the NSF (W.S.B.), the University of California at Santa Barbara (J.P.K.) and the Natural Science and Engineering Research Council of Canada (J.T.T.).

Stroboscopic NMR microscopy of the carotid artery

Ronald W. Behling*, Helen K. Tubbs*,
Michael D. Cockman & Lynn W. Jelinski†

AT&T Bell Laboratories, Murray Hill, New Jersey 07974, USA

* Present addresses: Squibb Institute for Medical Research, Princeton, New Jersey, NJ 08543, USA (R.W.B.) and Cornell Medical School, New York, 10021 USA (H.K.T.)

† To whom correspondence should be addressed

THE non-invasive measurement of vascular dynamics and elasticity is critical in understanding haemodynamic conditions of cardiovascular diseases such as hypertension and atherosclerosis¹. Although there are numerous invasive and *in vitro* techniques² for such measurements, until now non-invasive methods have been limited³. We have now obtained stroboscopic NMR images^{4,5} of the carotid arteries of 80-g rats. The change in the cross-sectional area of arteries of diameter ~600–800 μm was correlated with the change in absolute blood pressure. These are the first microimages^{6–9} of a dynamic system and enable the direct visualization of compliance, the non-invasive measurement of Young's modulus, the direct determination of the local effects of vasoconstrictors and vasodilators and the mapping of the entire cardiac cycle.

Figure 1 (left panel) shows a large-field-of-view (FOV) spin-echo NMR image of the left side of the neck of an 80-g rat, whereas the images shown in the middle and right panels correspond to systole and diastole, respectively. The carotid artery at systole appears dark (corresponding to the absence of signal) because the blood that was excited during slice selection had flowed out of the slice by the time the echo was obtained. Fresh

unexcited blood had taken its place, thereby affording great contrast. The image at diastole is an extreme example of a complete loss of contrast that occurs when the blood flow is so slow that it is difficult to distinguish between the blood in the artery and the water in the surrounding tissue. This effect was observed only rarely (more representative images at diastole are shown in Fig. 3), and the echo time (T_E) could be adjusted to change the intensity of the blood signal in the artery.

Data such as these shown in Fig. 1 were analysed by drawing expanded plots, the contours of which correspond to the grey levels in the image. Representative plots are shown in Fig. 2. Each of the areas of these plots was measured independently by three individuals, using a planimeter. The averages of the three normalized measurements for two rats are shown in Fig. 3. The error bars correspond to the standard error of the three separate measurements. The error is small near systole (~2%) and larger near diastole (~8%) because of the flow effects mentioned above.

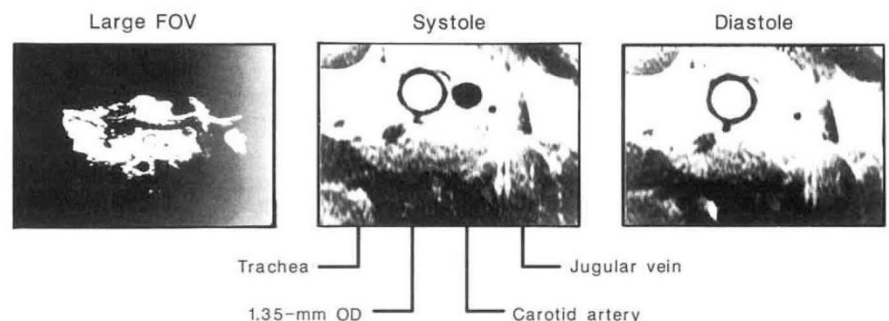
The cross-sectional areas of the carotid artery at the extremes of systole and diastole can be correlated with the absolute blood pressure to determine the distensibility, related to the compliance, of the carotid artery. Compliance is defined as the volume change per unit of pressure; our measurements, however, recorded a change in the cross-sectional area. We have assumed that the length of the carotid artery did not change appreciably during the heart cycle, an assumption that is valid in view of separate measurements of the transverse and longitudinal Young's modulus (see below). The distensibility is calculated by:

$$\frac{(A_{\text{systole}} - A_{\text{diastole}}) / A_{\text{diastole}}}{P_{\text{systole}} - P_{\text{diastole}}} \times 100\%$$

where P_{systole} and P_{diastole} are the absolute blood pressures at systole and diastole, respectively, and A_{systole} and A_{diastole} are

FIG. 1 Spin-echo NMR images of the left side of the neck of an 80-g rat. Left, Field of view (FOV) 33.9 × 33.9 mm; middle, FOV 8.5 × 8.5 mm; this image corresponds to systole. Right, FOV 8.5 × 8.5 mm; image corresponds to diastole.

METHODS. Female Sprague-Dawley rats (80 g) were anaesthetized with ethyl carbamate (urethane, Sigma) in 0.85% saline (w/v) by injecting 850 mg of the solution per kg (body weight) intraperitoneally, and then injecting 850 mg per kg subcutaneously behind the neck. The rats were intubated and a water-filled capillary (1.0 mm × 1.35 mm o.d.) was inserted near the carotid artery as a marker for vertical positioning. The incision was sutured and electrocardiograph leads were placed on the upper abdomen, away from the surface coil, with the resultant electrocardiogram producing a V_3 -like trace. The rat was placed head-down in a specially designed plastic rodent holder that was affixed to the probe. The temperature of the rats decreased to 31 °C and stabilized at that level. They breathed 60% O_2 and 40% N_2 . The NMR images were obtained using a Bruker AM 360 equipped with an NMR microscope accessory. The probe circuit was modified to accommodate a 1.4-cm-diameter single-turn surface coil. A 2-ms lobeless sinc pulse was used for the slice-selective 90° and 180° pulses. The water line-width was shimmed on the desired slice to ~100 Hz. The gradient strengths for the 33.9 × 33.9 × 0.8-mm FOV were 0.69, 0.74 and 1.8 gauss cm^{-1} for the



read-out (x), phase encode (y) and slice select (z) directions, respectively. For the 8.5 × 8.5 × 0.8-mm FOV the gradient strengths were 2.77, 1.48 and 1.8 gauss cm^{-1} , respectively. The images consisted of two scans at each of 64 phase-encode increments surrounding the echo maximum. The pixel size in the phase-encode direction was 132 μm, and 33 μm in the read direction before zero filling. The data matrix was zero filled to 512 × 512 before Fourier transformation; no signal enhancement or digital filtering was applied to the data. Slice thickness was ~800 μm. The repetition time (T_R) was 6 s and the echo time (T_E) was 20 ms.